Fire Safety Journal 91 (2017) 768–775

Contents lists available at ScienceDirect

Fire Safety Journal

journal homepage: www.elsevier.com/locate/firesaf

IAFSS 12th Symposium 2017

Mapping areas at elevated risk of large-scale structure loss using Monte Carlo simulation and wildland fire modeling

Chris Lautenberger

Reax Engineering Inc., 1921 University Ave., Berkeley, CA 94704, United States

ARTICLE INFO

Keywords:
Modeling
Wildfires
Risk assessment

ABSTRACT

This work presents, and demonstrates through application to California, a data-driven methodology that can be used to identify areas at elevated risk of experiencing wildland fires capable of causing large-scale structure loss. A 2D Eulerian level set fire spread model is used as the computational engine for Monte Carlo simulation with ignition points placed randomly across the landscape. For each randomly-placed ignition point, wind and weather conditions are also selected randomly from a 10-year climatology that has been developed by others using the Weather Research and Forecasting (WRF) mesoscale weather model at a resolution of 2 km. Fuel and topography inputs are obtained from LANDFIRE. Housing density is estimated from 2010 Census block data. For each randomly-selected combination of ignition location and wind/weather, fire progression is modeled so that fire area and number of impacted structures can be recorded. This is repeated for over 100 million discrete ignition points across California to generate “heat maps” of fire probability, fire consequence, and fire risk. In this work, fire volume (spatial integral of burned area and flame length) is used as a proxy for fire probability since quickly spreading fires with large flame lengths are most likely to escape initial attack and become extended attack fires. Fire consequence is taken as the number of impacted structures. Fire risk is then estimated as the product of probability and consequence. The methodology is assessed comparing the resultant fire risk raster with perimeters from California's 20 most damaging fires as tabulated by the California Department of Forestry and Fire Protection (CALFIRE). It is found that these historical perimeters from damaging fires correlate well with areas identified as high risk in the Monte Carlo simulation, suggesting that this methodology may be capable of identifying areas where similarly damaging fires may occur in the future.

1. Introduction – wildland fire risk

The primary goal of this work is to describe and demonstrate a data-driven methodology that can be used to quantify wildland fire risk across large geographical areas. Wildland fire hazard or risk mapping can be divided into short-term and long-term analyses. Short-term fire hazard/risk is strongly correlated to current weather conditions and may be used for suppression planning and/or resource allocation. Long-term fire hazard/risk mapping involves factors that change on a longer temporal scale. The emphasis of this paper is long-term wildland fire risk mapping.

The term *fire risk* is often used inconsistently and the meaning of this term in the wildland fire literature is sometimes different from its meaning in other branches of science and engineering. To avoid confusion, and to explicitly identify what this work quantifies, the meaning of *wildland fire risk* within the context of this work is explained below.

Hardy [1] proposed the following definition of *fire risk*, indicating there is broad agreement on this definition among US and international organizations:

Fire risk: The chance that a fire might start, as affected by the nature and incidence of causative agents.

This definition is problematic for practical wildland fire risk mapping, as illustrated by a simple thought experiment: Consider a plot of cured grass with low fine fuel moisture, surrounded on three sides by a fire break and on the remaining side by a busy highway. Under Hardy's definition above [1], fire risk would be high because there is a high probability of ignition. However, the negative consequences of such a fire are minimal because it would be contained by fire breaks with no impact to the built environment or life safety.

For consistency with the use of the term *risk* in the risk analysis literature, the following definitions of *risk* and *wildland fire risk* proposed by Bachman and Allgöwer [2] are adopted here:

Risk: The probability of an undesired event and its outcome. An undesired event is a realization of a hazard.

> *Wildland fire risk*: The probability of a wildland fire occurring at a specified location and under specific circumstances, together with its expected outcome as defined by its impacts on the objects it affects.

These definitions are consistent with conventional definitions of *risk*, which is usually taken as an event's probability multiplied by its

http://dx.doi.org/10.1016/j.firesaf.2017.04.014
Received 10 February 2017; Received in revised form 5 April 2017; Accepted 6 April 2017
Available online 08 May 2017
0379-7112/

potential negative consequences or impacts. High probability of occurrence does not necessarily indicate high fire risk if values at risk (structures, timber, *etc.*) are unaffected [3].

2. Previous uses of Monte Carlo simulation to quantify wildland fire risk

Different approaches to quantifying wildland fire risk may be appropriate under different circumstances. Wildland fire hazard/risk assessment using fire behavior modeling and Monte Carlo simulation has recently seen increased usage due in part to more powerful computational resources, improved fire models, and readily available geospatial input data. ArcFuels [4,5] provides a desktop-based interface between ArcGIS and widely-used fire behavior models such as FARSITE [6] and FLAMMAP [7].

Keane et al. [8] highlighted the potential for Monte Carlo simulation to be used for wildland fire risk quantification, stating "Andrews (2007) FSPRO approach in which maps of fire intensity distributions are computed from thousands of FARSITE runs is perhaps the most significant step towards fine scale risk mapping." Such approaches can capture fire shadows, islands, and related effects. These spatial effects cannot be captured by analyses that consider conditions only at a point, or burn every point as a head fire, but would be captured by analyses that include fire progression. For these reasons, Monte Carlo simulations wherein fire spread is modeled from tens of thousands of separate ignition locations under a range of weather conditions is one of the most promising tools for quantitative wildland fire risk/hazard assessment.

Carmel et al. [9] conducted a Monte Carlo simulation using hundreds of FARSITE [6] simulations to assess fire risk in a 300 km^2 area near Mt. Carmel in Northwestern Israel. Weather inputs were developed from three nearby weather stations and standard fuel models were adapted for local conditions. 500 FARSITE [6] simulations were conducted and used to generate a heat map that identified hot spots and cold spots corresponding to the number of times that a particular location was burned by the simulated fires, which can be thought of as being analogous to fire frequency. The Carmel et al. study was published in 2009 [9]; tragically, in December 2010, a 2180 ha fire burned through the Mt. Carmel area, causing 45 deaths. This provided an unfortunate but unique opportunity for the authors to assess their pre-fire risk map [9] in a post-fire study [10]. It was concluded that most of the areas burned in the 2010 fire corresponded to high risk levels in the pre-fire risk map [10].

Ager, Finney, and McMahan [11] indicate that the actuarial definition of wildfire risk is "the expected net value change calculated as the product of (1) probability of a fire at a specific intensity and location, and (2) the resulting change in financial or ecological value." Based on that definition, they developed a modeling framework that can be used to calculate the net value change for fire events of varying severity. Their modeling process involved three separate steps: 1) Applying the Forest Vegetation Simulator/Parallel Processing Extension to simulate the effect of various landscape fuels treatments; 2) Using FLAMMAP to calculate elliptical fire spread dimensions, and 3) Applying RANDIG to simulate propagation of randomly ignited fires. Monte Carlo simulation was used to investigate the differences in net value change attributed to the different loss functions, fuels treatment types, and treatment areas.

Monte Carlo simulation has been used in Australia to quantify fire risk associated with overhead electrical utilities. This work was motivated by the 7 February 2009 Black Saturday Fires when hot dry winds led to ignition and rapid spread of several powerline-ignited fires in Victoria, ultimately resulting in over 150 fatalities and the loss of thousands of structures. The Powerline Bushfire Safety Program subsequently commissioned a project to identify powerline fire ignition points likely to result in high fire consequence to target investment in areas of highest bushfire risk. PHOENIX RapidFire [12–16] was used to simulate fire spread from multiple ignition points under specific weather conditions consistent with Ash Wednesday / Black Saturday. The primary output was an estimate of the number of homes burned by a powerline-ignited fire starting at a particular location.

One of the most ambitious applications of Monte Carlo analysis to quantify wildland fire hazard/risk was recently conducted in California [17]. The California Public Utilities Commission (CPUC) directed an Independent Expert Team (IET), led by the California Department of Forestry and Fire Protection (CAL FIRE), to develop a statewide map that identifies "the fundamental physical and environmental features that lead to an elevated likelihood of overhead utility facilities initiating fires that are then likely to lead to large and damaging wildfires" [17]. The IET developed a 10-year climatology using the Weather Research and Forecasting (WRF) model [18,19] to provide statewide hourly wind/weather fields at 2 km resolution. These weather inputs were used to drive a statewide Monte Carlo fire spread analysis involving over 100 million randomly distributed ignition points. Fire progression was simulated using GridFire [20], a raster-based fire spread model similar to HFire [21]. Their work [17] was mirrored by the author using ELMFIRE [22,23] (Eulerian Level Set Model for Fire Spread) in his capacity as a subject matter expert for several electrical utilities and telecommunications firms. The present paper is based on this earlier work, with the important enhancement that fire consequence is quantified based on the number of impacted structures.

3. Current use of Monte Carlo simulation to quantify wildland fire risk

Monte Carlo simulation has shown great promise for quantifying wildland fire risk. This section describes how Monte Carlo simulation is used to quantify wildland fire risk in the current work.

3.1. Fire spread model: ELMFIRE

The open source fire spread model ELMFIRE [22,23] is used here as the computational engine for Monte Carlo simulation of fire risk. ELMFIRE uses a narrow-band Eulerian level set method [24] – a technique capable of tracking curved surfaces on a regular grid – to model fire edge propagation. ELMFIRE is similar to other two-dimensional fire simulators such as FARSITE [6] or PHOENIX RapidFire [12–16] in that it calculates surface fire spread rate using the Rothermel surface spread model [25,26] and applies Huygens' Principle such that each point along the fire front behaves as an independent elliptical wavelet [27] with length to breadth ratio determined semi-empirically [6,28]. ELMFIRE simulates transition from surface to crown fire using the Van Wagner criterion [29]. Passive/active crown fire spread rates are estimated from Cruz et al. [30]. Surface fire flame length is calculated from fireline intensity using Byram's fire intensity equation. Flame length from burning crowns is similarly calculated after estimating the contribution to fireline intensity from crown fire. Although enhanced rates of spread associated with passive / active crown fire are included in the simulations, spot fire formation by firebrand lofting caused by torching/crowning is not. However, areas likely to trigger spot fires are implicitly captured in the analysis via the fire volume metric that will be described later because areas where passive/active crown fire occur also experience faster rates of spread, longer flame lengths, and larger fire volumes. ELMFIRE is parallelized using Message Passing Interface (MPI) so that it can be deployed across standard large-scale computational resources. On a 128-core cluster, over 50 million hours of fire progression can be simulated per day.

To provide the reader with some understanding of the types of ELMFIRE outputs that will be used later in this work, Fig. 1 shows 24-h of fire progression from an individual ignition site as modeled with ELMFIRE. In this example, fire area at the conclusion of the simulation is approximately 225 ha. The black contour lines in Fig. 1 represent fire

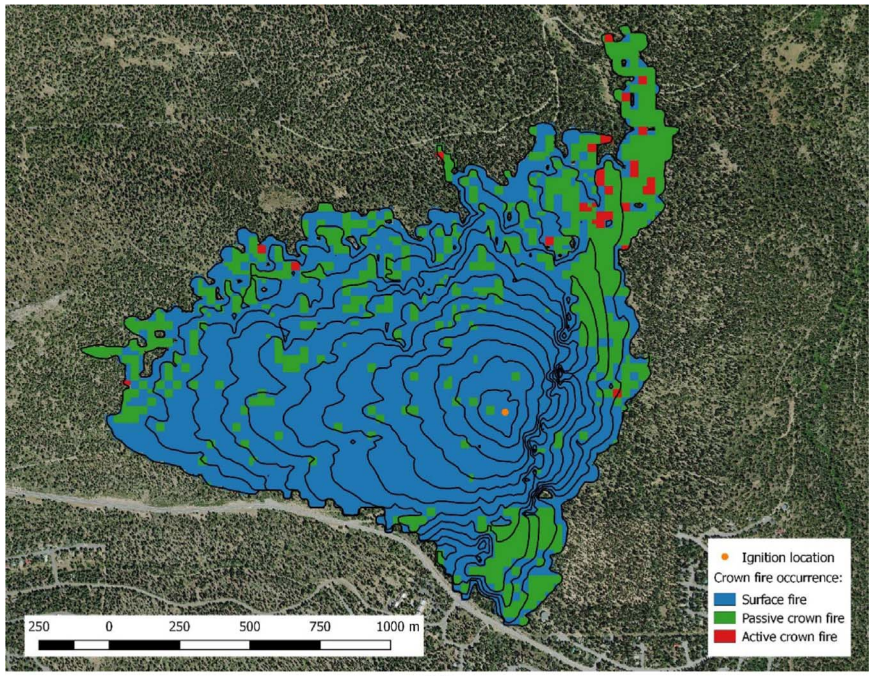

(a)

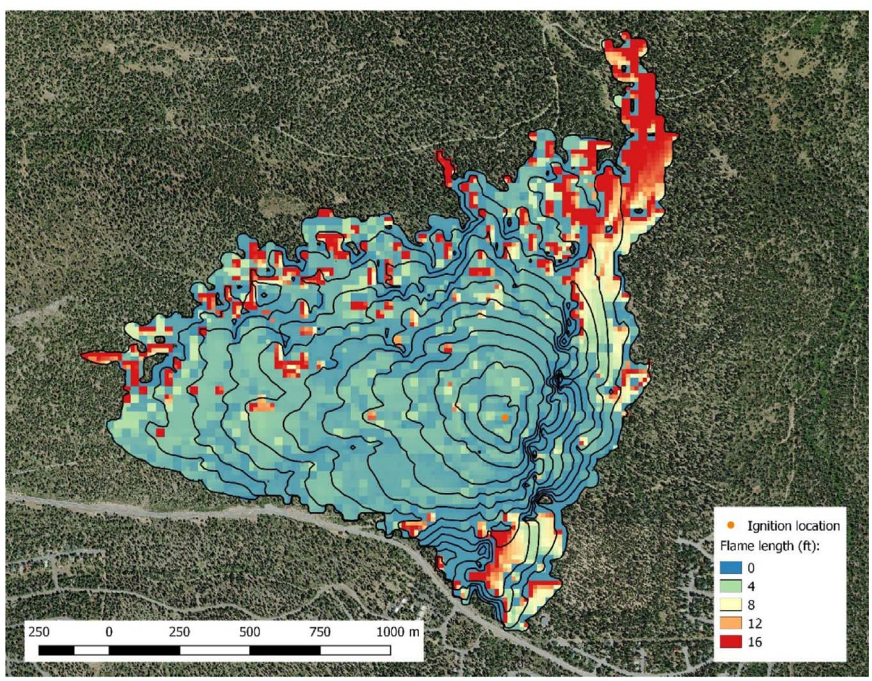

(b)

Fig. 1. Sample ELMFIRE fire spread simulation for individual fire ignition. (a) Fire type (surface fire, passive crown fire, or active crown fire). (b) Flame length. (For interpretation of the references to color in this figure, the reader is referred to the web version of this article.)

front position at 2-h intervals. Fig. 1a also shows which parts of the burned area experienced surface fire (blue), passive crown fire (green), or active crown fire (red). Fig. 1b shows fire perimeter contours and flame length variation within the fire perimeter. Flame length is highest in areas that burn as heading fires or those that experience crown fire, and lowest in areas that burn as a flanking or backing fire or as a surface fire. Fire "volume" (a concept used later as a proxy for the relative likelihood that a fire escapes initial containment efforts) is calculated by pixel-wise integration of the burned area multiplied by flame length (i.e., as shown graphically in Fig. 1b).

Ignition locations are distributed randomly at a density of 1000 ignitions per each 2 km WRF cell (i.e., 250 ignitions per square kilometer). Since California covers approximately 425,000 square kilometers, this ignition density corresponds to over 100 million separate ignitions statewide. Analyses have been conducted at higher ignition densities with no statistically significant results. For each randomly selected ignition location, wind and weather conditions are also randomly selected as described in the next section, and used to drive a one-hour fire spread simulation.

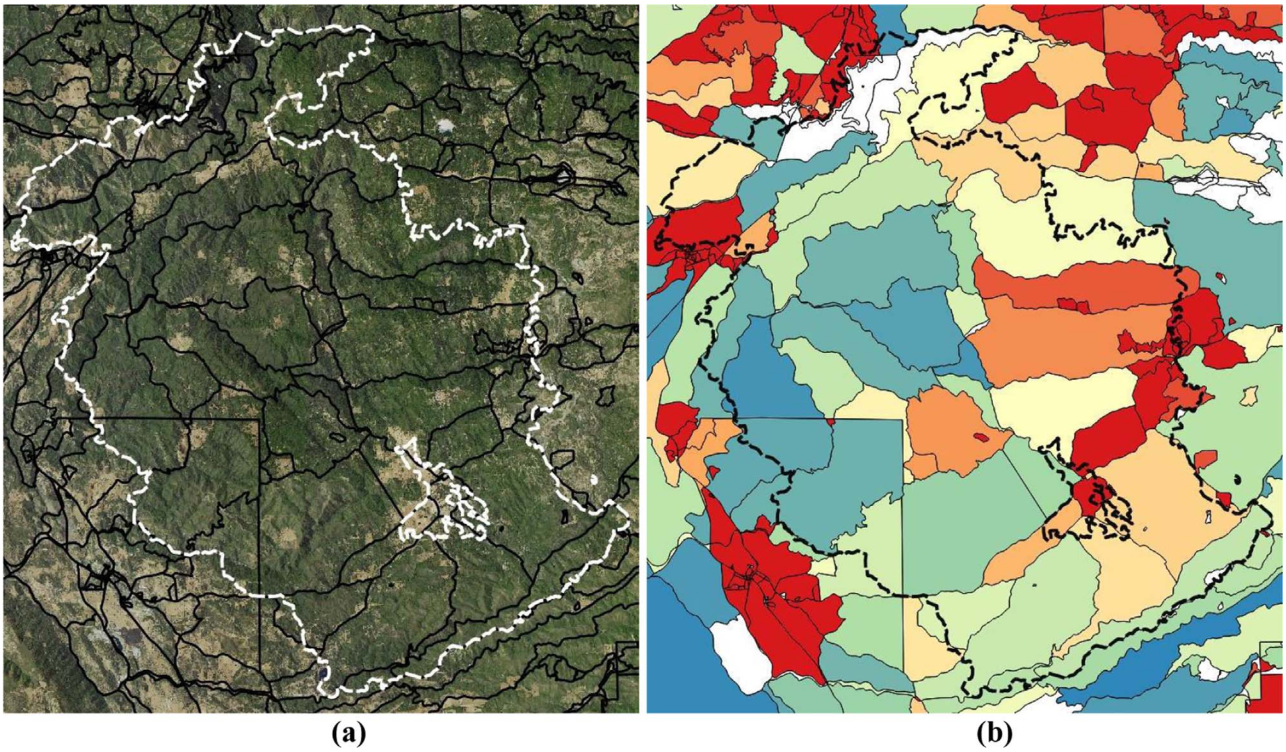

Fig. 2. Butte Fire footprint (dash line). (a) Census blocks (solid lines) on orthoimagery. (b) Housing density (structures/km^2) colored from 0 (blue) to > 75 (red). (For interpretation of the references to color in this figure legend, the reader is referred to the web version of this article.)

3.2. Wind and weather

As part of the above-mentioned work to identify areas of California at elevated risk of experiencing damaging powerline fires, a 10-year (2004–2013) climatology was developed by others [17] using the Weather Research and Forecasting (WRF) model [18,19] at 2 km resolution. This climatology includes 87,672 hourly records (24 h per day multiplied by 365 days per year plus 3 leap days) for each 2 km pixel. This climatology includes hourly fields of wind speed and direction, relative humidity, temperature, precipitation, and solar insolation. 1-h, 10-h, and 100-h dead fuel moistures were calculated from relative humidity and temperature fields using timelag theory [31]. Since most records in the climatology are unremarkable from a fire weather standpoint, a smaller subset of hourly records was extracted to drive Monte Carlo Simulation as described further below.

For each hourly record in each pixel, Fosberg Fire Weather Index (FFWI) [32] was calculated from wind speed, relative humidity, and temperature. FFWI is a nonlinear filter that combines these quantities into a single measure of fire spread potential based on instantaneous meteorological/wind conditions, but it does not consider drought, recent precipitation, or atmospheric instability. For each pixel, the daily maximum FFWI was determined for each of the 3653 days in the climatology. Then, the 3653 daily maximum FFWI values were sorted from high to low, while carrying along all other quantities (including temperature, relative humidity, wind speed, and wind direction). For each pixel, weather records corresponding to the top 3% (or 112 hourly records) of the daily maximum FFWI values are used to drive the Monte Carlo simulation. The top 3% was chosen because fire behavior analyses are commonly conducted based on fire 97th percentile (or higher) fire weather. Each fire simulation is driven by a single hourly record from the top 3% of the FFWI-sorted climatology.

3.3. Fuel and topography

Fuel and topography input layers were obtained from the LANDFIRE 2012 (LANDFIRE 1.3.0) database [33,34] at a resolution of 30 m. Topography layers include elevation, slope, and aspect. Fuel layers include surface fuel model (in the Scott and Burgan 40 system [35]), canopy height, canopy cover, canopy base height, and canopy bulk density. The surface fuel layer was modified to correct known fuel assignment errors in LANDFIRE using the methodology described by Sapsis et al. [17]. Static fields of live woody fuel moistures were estimated from the National Live Fuel Moisture Database [36] at a resolution of 20 km for the months of June – September. Live herbaceous fuels are assumed to be fully cured (30% moisture content), and foliar moisture content is assumed constant at 90%.

3.4. Assets at risk

Within the context of wildland fire, both positive and negative outcomes can be realized from a given fire [3]. A low-intensity fire occurring within the historic range of variability may provide a net benefit to the burned areas. However, this is not likely to be true for fires burning under extreme fire weather conditions (high wind, low humidity) in areas adapted to low intensity/high frequency fire. It is also unlikely to be true for fires burning through intermix or interface areas with structures. In this work, negative fire consequences/impacts are taken as negative impacts to structures. Although other impact categories such as timber, natural resources, critical infrastructure, fire suppression costs, or loss of non-market environmental services could potentially be included, most of these are difficult to quantify. Consequently, this work addresses only impact to structures and not loss of other assets at risk.

The first step in modeling fire impacts to structures is development of a data set that identifies locations of structures. US Census data were used to calculate population and housing density at the census block level. Given that California's ~425,000 km^2 area is divided among 710,145 census blocks, this provides a reasonably fine-grained state-wide view of structure locations.

2010 US Census data for California were obtained in GIS (shapefile) format [37,38]. Housing density (structures/km^2) was calculated for each census block polygon in California by dividing the housing count for each census block by its area. Each polygon, and the resultant housing density, were then burned to a raster having the same projection and resolution (30 m) as the underlying fuels inputs.

An example of this structure density calculation is shown graphically in Fig. 2. The dashed line is the outline of the 2015 Butte Fire, which burned approximately 29,000 ha and destroyed approximately 550 homes and 370 outbuildings. In Fig. 2a, census blocks (black lines) are overlaid on orthoimagery. Fig. 2b shows housing density (structures/km^2) calculated for each census block. The values range from close to 0 (blue) to greater than 75 structures/km^2 (red). White polygons in Fig. 2b are Census blocks with zero housing density.

For each fire simulated with ELMFIRE, the total number of impacted homes is calculated by integrating burned area and housing density for each 30 m burned pixel within the fire perimeter. While this method cannot determine whether specific structures would be impacted by a fire, it captures average losses at the Census block level. For example, if a fire burns 1 km^2 of an area having a housing density of 20 structures per km^2, the total number of impacted structures as reported by ELMFIRE would be 20. Actual impacted structures would depend on the location of those structures in the census block relative to the fire edge.

It is noted that affected/impacted structures (i.e., those within the fire perimeter) as tabulated here does not necessarily correspond to damaged or destroyed structures. Post-fire inspection of neighborhoods that have experienced wildland urban interface fires typically reveals that many structures within the fire perimeter survive. Structure survivability is a complex function of defensible space, construction techniques, suppression efforts, etc. While others have attempted to model structure losses based on factors such as flame length or ember density, such methods have not been validated and may introduce a false sense of precision. For this reason, no such attempts are made here.

4. Quantifying wildland fire risk across California

Wildland fire risk is considered here to be "The probability of a wildland fire occurring at a specified location and under specific circumstances, together with its expected outcome as defined by its impacts on the objects it affects" [2]. This is similar to the classic definition of risk as probability times consequence. A California-wide measure of wildland fire risk is developed by upsampling Monte Carlo simulation results to facilitate analysis at statewide scales. Fire probability and consequence are then defined in terms of ELMFIRE outputs. Finally, fire probability and consequence are combined into a single statewide measure of fire risk and the resultant risk map is compared to historical damaging fires.

4.1. Upsampling Monte Carlo simulation results

Outputs from the Monte Carlo fire spread simulation are extremely fine grained. For each discrete ignition location (a 30 m by 30 m pixel) and wind/weather stream, ELMFIRE tabulates the resultant fire area, fire volume, and number of impacted structures. As an illustrative example, Fig. 3a shows individual ignition locations colored by the area of the fire that resulted from an ignition at that location. Fine-scale patterns, a result of combined influence of fuels/weather/topography, are apparent. When viewing risk at scales approaching the size of California, some degree of upsampling is necessary. It has been found that upsampling to pixels between 1 km and 2 km works well for statewide applications. Fig. 3b shows fire area data from Fig. 3a upsampled to 1 km (250 discrete ignition points per upsampled pixel, on average).

4.2. Quantifying fire probability and consequence

It has been estimated that approximately 95% of fire ignitions in California are anthropogenic [39]. Since population and infrastructure are not distributed uniformly across California, fire ignitions are also not uniformly distributed spatially. Although statistical identification of areas more likely to experience fire ignitions should be possible, doing so is a significant undertaking. To simplify the current analysis, it is assumed that ignitions are distributed uniformly. However, risk analysis still requires that a probability metric be defined. For that reason, the concept of probability of occurrence is replaced with probability that a fire escapes initial containment efforts. This is justified because most fires are controlled or extinguished while still small. It is a small percentage of fires – specifically those that escape initial containment efforts and become extended attack or campaign fires – that are responsible for the majority of hectares burned in California. Fires are most likely to escape initial containment when fuels, weather, and topography lead to rapid fire spread, long flame lengths, and spotting that hinder control operations. Therefore, fire volume (which combines fire area and flame length) is used here as a proxy for probability of fire escaping initial containment efforts. Fig. 4a shows fire volume colored by quantile and upsampled to 2 km resolution from the Monte Carlo fire spread simulation. This is considered a proxy for relative probability of fire escaping initial containment efforts. Quantiles are calculated such that each quantile bin contains the same number of 2 km pixels, e.g. the 95th quantile bin includes the top 5% of all pixels ranked by fire volume.

Fire consequence is taken here as fire's impact on the objects it affects. As described earlier, the only assets at risk continued here are homes from the US Census. Fig. 4b shows fire consequence colored by quantile (also upsampled to 2 km resolution) from the ELMFIRE Monte Carlo simulation. Comparison of Figs. 4a and b reveals very different large-scale spatial patterns. This is because Fig. 4a is a function of fuels, weather, and topography – without consideration of structures. However, Fig. 4b is essentially the intersection of fuels, weather, and topography with structures. It has similarities to Haas et al.'s [41] "National map of risk to populated places".

Fig. 4 shows probability and consequence for fires starting at specific locations because fire volume and impact to structures are tabulated for discrete ignition locations. This is somewhat different than using conditional burn probabilities to portray fire risk as is sometimes estimated from Monte Carlo simulations.

4.3. Quantifying fire risk

With probability and consequence now defined and quantified, fire risk is calculated as probability times consequence (essentially, Fig. 4a multiplied by Fig. 4b). Fig. 5 shows the resultant fire risk raster colored by quantile.

4.4. Comparison of calculated fire risk to historical damaging fire perimeters

CAL FIRE maintains a list of the 20 most damaging fires in California history [40]. That list is reproduced in Table 1. Note that the most damaging fires are not necessarily the largest. For example, the Tunnel (or Oakland Hills) Fire destroyed 2900 structures and caused 25 deaths, but burned only 650 ha (1600 acres). The Cedar Fire burned a similar number of structures as the Oakland Hills Fire, but the area burned by the Cedar Fire was over 150 times the area burned by the Oakland Hills Fire. This highlights the importance of assessing fire risk as the intersection of fuels, weather, topography, and structures.

As a qualitative assessment of the fire risk quantification methodology described herein, Fig. 6 shows perimeters corresponding to the 20 fires from Table 1 overlaid on the 80th quantile (top 20%) of 2 km fire risk pixels from Fig. 5. Owing to the relatively small size of these fires compared with the area of California, the comparison is somewhat difficult to view at statewide scales. However, viewing each individual

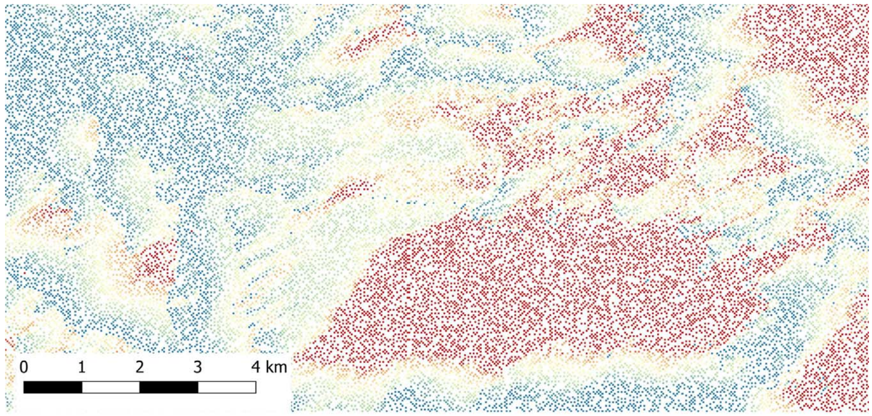

(a)

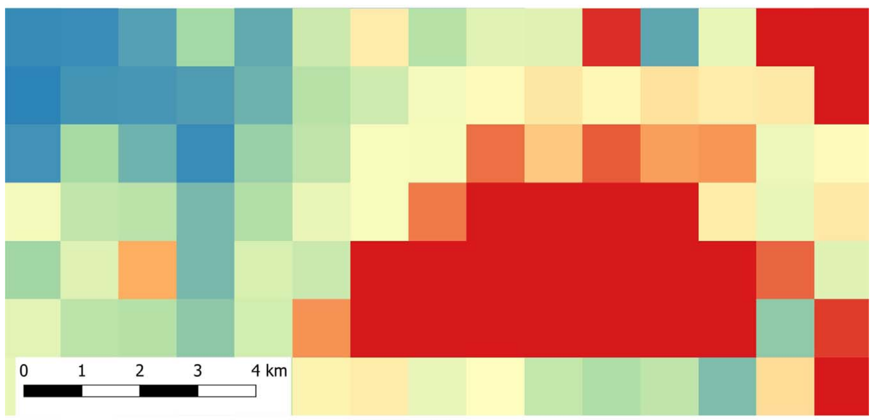

(b)

Fig. 3. Sample Monte Carlo simulation results – fire area. (a) No upsampling. (b) Upsampled to 1 km.

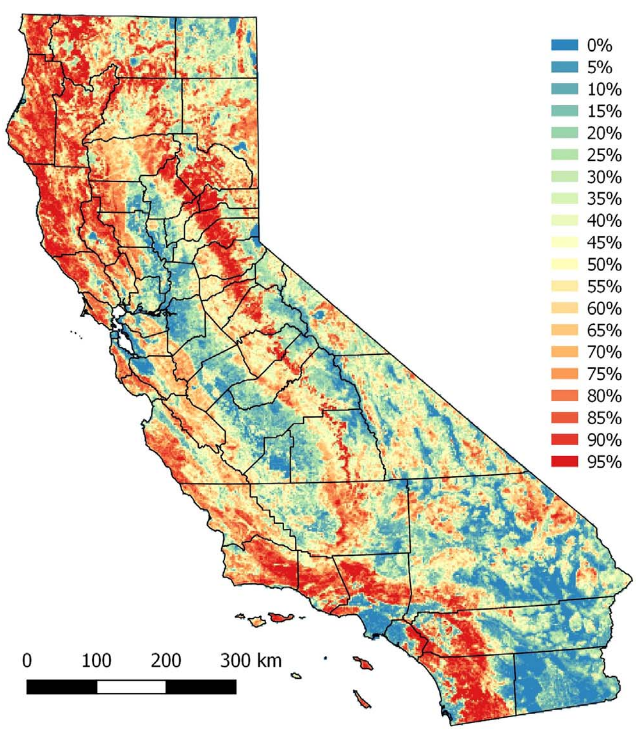

(a)

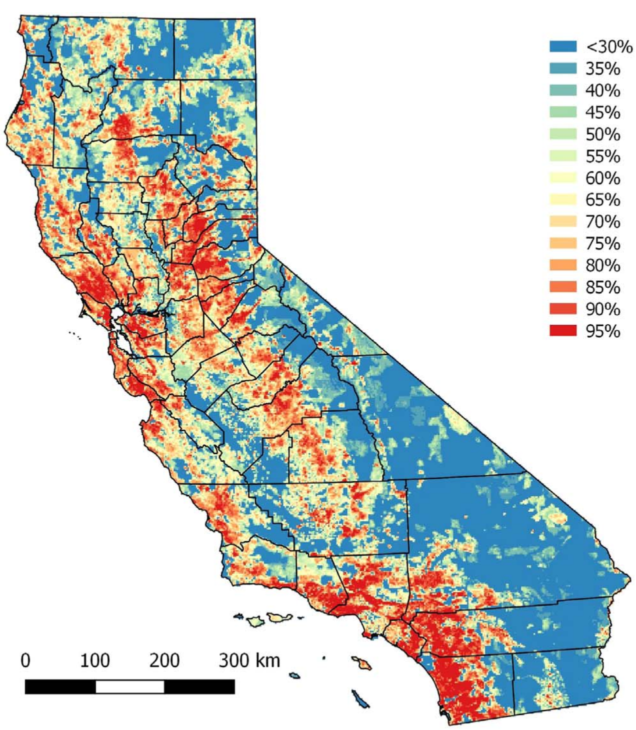

(b)

Fig. 4. California fire probability and consequence colored by quantile. (a) Fire volume as a proxy for relative probability of fire escaping initial containment. (b) Fire consequence (impact to homes).

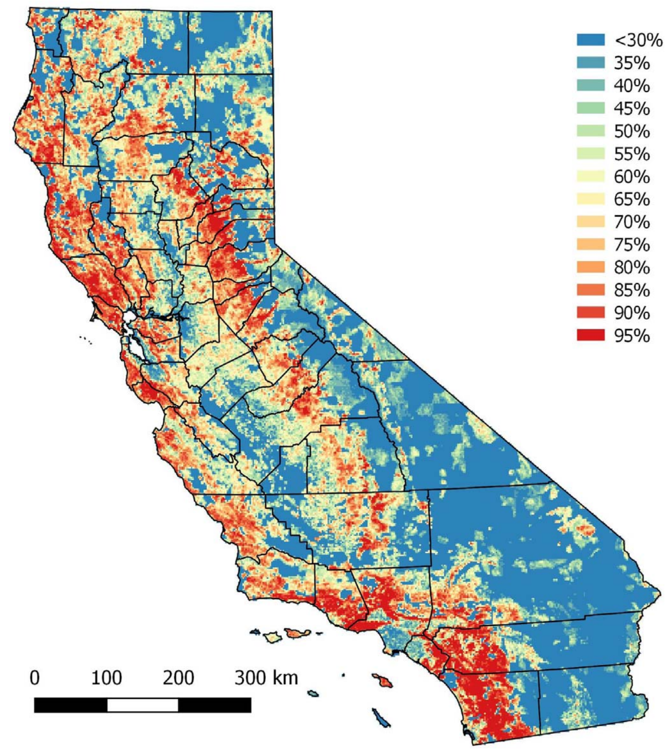

Fig. 5. California fire risk based on impact to homes colored by quantile.

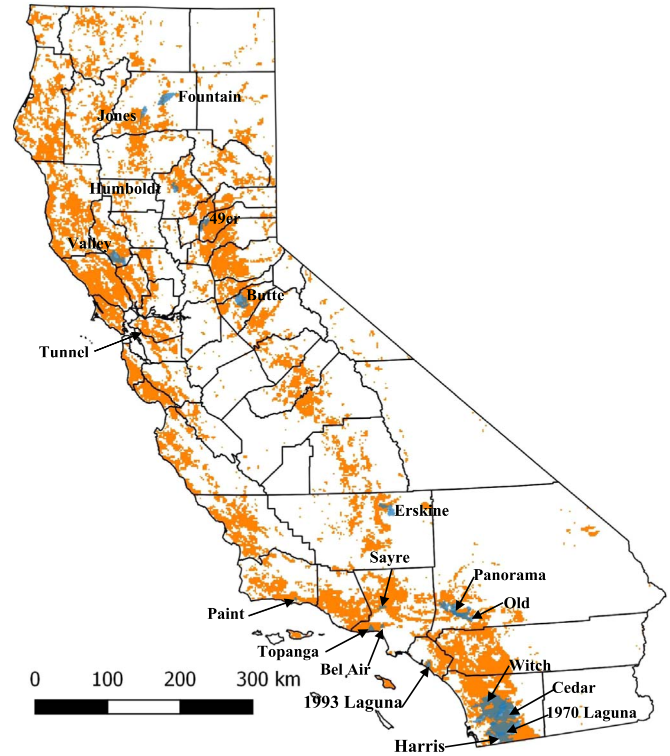

Fig. 6. 80th percentile of fire risk (orange) with perimeters from 20 most damaging fires in California [40] overlaid (semi-transparent blue). (For interpretation of the references to color in this figure legend, the reader is referred to the web version of this article.)

fire perimeter separately shows that every fire perimeter from the 20 most damaging list intersects the 80th risk quantile raster, with several perimeters contained entirely within the 80th risk quantile raster. This qualitative assessment suggests that this methodology may be capable of identifying areas where similarly damaging fires may occur in the future.

5. Concluding remarks

This paper demonstrates a data-driven methodology that uses Monte Carlo simulation and wildland fire modeling to identify areas at elevated risk of experiencing damaging wildland fires with the potential to destroy multiple structures. It is intended for application across large geographic areas, and the methodology is demonstrated through application to California. Comparison of areas identified as elevated risk with locations of the 20 most damaging fires in California shows a good qualitative correlation, suggesting that this methodology may be capable of identifying areas where similarly damaging fires may occur in the future.

There are several areas where this work could be refined or enhanced. An incomplete list includes:

Table 1
Top 20 most damaging fires as tabulated by CAL FIRE [40].

Fire Name (Cause)		Date	County	Acres	Structures	Deaths
1	Tunnel - Oakland Hills (Rekindle)	October 1991	Alameda	1600	2900	25
2	Cedar (Human Related)	October 2003	San Diego	273,246	2820	15
3	Valley (Under Investigation)	September 2015	Lake, Napa & Sonoma	76,067	1955	4
4	Witch (Powerlines)	October 2007	San Diego	197,990	1650	2
5	Old (Human Related)	October 2003	San Bernardino	91,281	1003	6
6	Jones (Undetermined)	October 1999	Shasta	26,200	954	1
7	Butte (Under Investigation)	September 2015	Amador & Calaveras	70,868	921	2
8	Paint (Arson)	June 1990	Santa Barbara	4900	641	1
9	Fountain (Arson)	August 1992	Shasta	63,960	636	0
10	Sayre (Misc.)	November 2008	Los Angeles	11,262	604	0
11	City of Berkeley (Powerlines)	September 1923	Alameda	130	584	0
12	Harris (Under Investigation)	October 2007	San Diego	90,440	548	8
13	Bel Air (Undetermined)	November 1961	Los Angeles	6090	484	0
14	Laguna (Arson)	October 1993	Orange	14,437	441	0
15	Erskine (Under Investigation)	June 2016	Kern	46,684	386	2
16	Laguna (Powerlines)	September 1970	San Diego	175,425	382	0
17	Humboldt (Arson)	June 2008	Butte	23,344	351	4
18	Panorama (Arson)	November 1980	San Bernardino	23,600	325	3
19	Topanga (Arson)	November 1993	Los Angeles	18,000	323	0
20	49ER (Illegal Debris Burning)	September 1988	Nevada	33,700	312	0

*"Structures" include homes, outbuildings (barns, garages, sheds, etc) and commercial properties.
**This list does not include fire jurisdiction. These are the Top 20 regardless of whether they were state, federal, or local responsibility.

- Development of ignition probability rasters based on anthropogenic and natural causes.
- Development of damage functions to quantify structure loss probability based on factors such as fireline intensity / flame length or ember density.
- Incorporation of damage functions to quantify impacts to values/ assets at risk in addition to structures (timber, natural resources, cultural relics, etc.).
- Incorporation of secondary factors that may affect the probability of fires escaping initial containment efforts or becoming large campaign fires including road density (km/km^2), distance from closest fire station(s) and/or air attack bases, and terrain ruggedness.
- Development of temporally contiguous climatological inputs to facilitate running fire spread simulations for longer durations such as one or two burn periods.
- Incorporation of fine-scale local knowledge that may not be captured in landscape-scale input layers. One such example is tree mortality (which has become widespread in California in recent years).
- This methodology quantifies fire risk associated with fires starting at a particular location on the landscape. However, conditional burn probabilities can also be calculated. This may be a more appropriate way to quantify fire risk at a particular location on the landscape.

Acknowledgements

Parts of this work have been shaped through insightful discussion with Dave Sapsis, David Saah, and Gary Johnson. Their contributions to this work are gratefully acknowledged. The climatology used in this work was developed by others (Ref. [17] and Tim Brown in particular).

References

[1] C.C. Hardy, Wildland fire hazard and risk: problems, definitions, and context, For. Ecol. Manag. 211 (2005) 73–82. http://dx.doi.org/10.1016/j.foreco.2005.01.029.
[2] A. Bachman, B. Allgöwer, A consistent wildland fire risk terminology is needed, Fire Manag. Today 61 (2001) 28–33.
[3] C. Miller, A. Ager, A review of recent advances in risk analysis for wildfire management, Int. J. Wildland Fire 22 (2013) 1–14. http://dx.doi.org/10.1071/WF11114.
[4] N.M. Vaillant, A.A. Ager, J. Anderson, L. Miller, ArcFuels User Guide and Tutorial: for Use with ArcGIS 9®, United States Department of Agriculture Forest Service, Pacific Northwest Research Station, General Technical Report PNW-GTR-877 June 2013.
[5] N.M. Vaillant, A.A. Ager, J. Anderson, ArcFuels10 System Overview, United States Department of Agriculture Forest Service, Pacific Northwest Research Station, General Technical Report PNW-GTR-875, March 2013.
[6] M.A. Finney, FARSITE: Fire Area Simulator – Model Development and Evaluation, United States Department of Agriculture Fire Service Rocky Mountain Research Station Research Paper RMRS-RP-4 Revised February 2004.
[7] M.A. Finney, An overview of FlamMap fire modeling capabilities, in Fuels Management–How to Measure Success, Ed. P.L. Andrews and B.W. Butler, Portland, OR, 2006.
[8] R.E. Keane, S.A. Drury, E.C. Karau, P.F. Hessburg, K.M. Reynolds, A method for mapping fire hazard and risk across multiple scales and its application in fire management, Ecol. Model. 221 (2010) 2–18. http://dx.doi.org/10.1016/j.ecolmodel.2008.10.022.
[9] Y. Carmel, S. Paz, F. Jahashan, M. Shoshany, Assessing fire risk using Monte Carlo simulations of fire spread, For. Ecol. Manag. 257 (2009) 370–377. http://dx.doi.org/10.1016/j.foreco.2008.09.039.
[10] S. Paz, Y. Carmel, F. Jahashan, M. Shoshany, Post-fire analysis of pre-fire mapping of fire risk: a recent case study from Mt. Carmel (Israel), For. Ecol. Manag. 262 (2011) 1184–1188. http://dx.doi.org/10.1016/j.foreco.2011.06.011.
[11] A. Ager, M. Finney, A. McMahan, A Wildfire Risk Modeling System for Evaluating Landscape Fuel Treatment Strategies, USDA Forest Service Proceedings RMRS-P-41. 149-162 (2006).
[12] K.G. Tolhurst, B. Shields, D. Chong, Phoenix: development and application of a bushfire risk management tool, Aust. J. Emerg. Manag. 23 (2008) 47–54.
[13] D. Chong, K. Tolhurst, T. Duff, Incorporating Vertical Winds into PHOENIX RapidFire's Ember Dispersal Model, Technical Report, Bushfire CRC/University of Melbourne, {C}14 December 2012{C}.
[14] D. Chong, K. Tolhurst, T. Duff, PHOENIX RapidFire 4.0′s Convective Plume Model, Technical Report, Bushfire CRC/University of Melbourne, 16 December 2012.
[15] D. Chong, K. Tolhurst, T. Duff, PHOENIX RapidFire 4.0 Convection and Ember Dispersal Model, Technical Report, Bushfire CRC/University of Melbourne, 16 December 2012.
[16] D. Chong, K. Tolhurst, T. Duff, B. Cirulis, Sensitivity Analysis of PHOENIX RapidFire, Technical Report, Bushfire CRC/University of Melbourne, 7 May 2013.
[17] D. Sapsis, T. Brown, C. Low, M. Moritz, D. Saah, B. Shaby, Mapping Environmental Influences on Utility Fire Threat. A Report to the California Public Utilities Commission Pursuant to R.08 – 11-005 AND R.15-05-006, Final Report, 16 February 2016.
[18] W.C. Skamarock, J.B. Klemp, A time-split nonhydrostatic atmospheric model for weather research and forecasting applications, J. Comput. Phys. 227 (2008) 3465–3485. http://dx.doi.org/10.1016/j.jcp.2007.01.037.
[19] 〈http://www.wrf-model.org/index.php〉.
[20] 〈https://github.com/sig-gis/gridfire〉.
[21] M.E. Morais, Comparing Spatially Explicit Models of Fire Spread Through Chaparral Fuels: A New Algorithm Based Upon the Rothermel Fire Spread Equation (MA Thesis), University of California at Santa Barbara, 2001.
[22] C. Lautenberger, Wildland fire modeling with an Eulerian level set method and automated calibration, Fire Saf. J. 62 (2013) 289–298. http://dx.doi.org/10.1016/j.firesaf.2013.08.014.
[23] 〈http://reaxengineering.com/trac/elmfire〉.
[24] J.A. Sethian, A fast marching level set method for monotonically advancing fronts, Proc. Natl. Acad. Sci. USA 93 (1996) 1591–1595.
[25] R.C. Rothermel, A Mathematical Model for Predicting Fire Spread in Wildland Fuels, USDA Forest Service, Research Paper International-115, January 1972.
[26] F.A. Albini, Estimating Wildfire Behavior and Effects, USDA Forest Service General Technical Report International-30, 1976.
[27] G.D. Richards, A general mathematical framework for modelling two-dimensional wildland fire spread, Int. J. Wildland Fire 5 (1995) 63–72. http://dx.doi.org/10.1071/WF9950063.
[28] H.E. Anderson, Predicting wind-driven wild land fire size and shape, United States Department of Agriculture Forest Service, Intermountain Forest and Range Experiment Station, Research Paper INT-RP-305, 1983.
[29] C.E. Van Wagner, Conditions for the start and spread of crown fire, Can. J. For. Res. 7 (1977) 23–34. http://dx.doi.org/10.1139/x77-004.
[30] M.G. Cruz, M.E. Alexander, R.H. Wakimoto, Development and testing of models for predicting crown fire rate of spread in conifer forest stands, Can. J. For. Res. 35 (2005) 1626–1639. http://dx.doi.org/10.1139/x05-085.
[31] A.J. Simard, The Moisture Content of Forest Fuels – 1. A Review of the Basic Concepts, Canadian Department of Forest and Rural Development, Forest Fire Research Institute, Information Report FF-X-14, Ottawa, Ontario, 47 pp.
[32] M.A. Fosberg, Weather in Wildland Fire Management: The Fire Weather Index, Conference on Sierra Nevada Meteorology, American Meteorological Society, pp 1–4 (1978).
[33] M.G. Rollins, LANDFIRE: a nationally consistent vegetation, wildland fire, and fuel assessment, Int. J. Wildland Fire 18 (2009) 235–249. http://dx.doi.org/10.1071/WF08088.
[34] 〈http://landfire.cr.usgs.gov/viewer/〉.
[35] J.H. Scott, R.E. Burgan, Standard Fire Behavior Fuel Models: A Comprehensive Set for Use with Rothermel's Surface Fire Spread Model 15, United States Department of Agriculture Forest Service, Rocky Mountain Research Station, 2005.
[36] 〈http://www.wfas.net/index.php/national-fuel-moisture-database-moisture-drought-103〉.
[37] 〈http://www2.census.gov/geo/tiger/TIGER2010/TABBLOCK/2010/tl_2010_06_tabblock10.zip〉.
[38] 〈ftp://ftp2.census.gov/geo/tiger/TIGER2010BLKPOPHU/tabblock2010_06_pophu.zip〉.
[39] A.D. Syphard, V.C. Radeloff, J. Keeley, T.J. Hawbaker, M.K. Clayton, S.I. Stewart, R.B. Hammer, Human influence on California fire regimes, Ecol. Appl. 17 (2007) 1388–1402. http://dx.doi.org/10.1890/06-1128.1.
[40] 〈http://www.fire.ca.gov/communications/downloads/fact_sheets/Top20_Damaging.pdf〉.
[41] J.R. Haas, D.E. Calkin, M.P. Thompson, A national approach for integrating wildfire simulation modeling into wildland urban interface risk assessments within the United States, Landscape Urban Plan. 119 (2013) 44–53. http://dx.doi.org/10.1016/j.landurbplan.2013.06.011.